ITS UCDAVIS
INSTITUTE OF TRANSPORTATION STUDIES

Past and Future Land Use Impacts of Canadian Oil Sands and Greenhouse Gas Emissions

January 2015

Sonia Yeh
Anqi Zhao
Sean D. Hogan
Adam R. Brandt
Jacob G. Englander
David W. Beilman
Michael Q. Wang

Institute of Transportation Studies ◦ University of California, Davis

1605 Tilia Street ◦ Davis, California 95616

PHONE (530) 752-6548 ◦ FAX (530) 752-6572

www.its.ucdavis.edu

Past and Future Land Use Impacts of Canadian Oil Sands and Greenhouse Gas Emissions

S. Yeh[a], A. Zhao[a], S. Hogan[b], A.R. Brandt[c], J.G. Englander[c], D.W. Beilman[d], M.Q. Wang[e]

[a] Institute of Transportation Studies, University of California, Davis, CA USA 95060.

[b] Geography Graduate Group, University of California, Davis, CA USA 95060.

[c] Department of Energy Resources Engineering, Stanford University, Stanford, CA USA 94305-2220.

[d] Department of Geography, University of Hawaii at Mānoa, Honolulu, HI, USA 96822.

[e] Systems Assessment Group, Energy Systems Division, Argonne National Laboratory, Lemont, IL 60439.

Corresponding author: Sonia Yeh, Institute of Transportation Studies, 1605 Tilia Street, University of California, Davis, CA USA 95060. Tel: (530) 830 2544; Email: slyeh@ucdavis.edu

Abstract.

The Canadian oil sands underlie 142,000 km^2 of the boreal forest in northeastern Alberta. Oil sands production greenhouse gas (GHG) emissions increased from 15 million tonnes (Mt) to 55 Mt between 1990 and 2011. Their production represents the fastest-growing source of GHG emissions in Canada. A large body of studies show that oil sands industries have large environmental impacts, including effects on climate, land, water, and air quality but GHG emissions from oil sands land use disturbance and future land use impacts have yet to be examined in detail and the associated literature is scarce and incomplete. Our paper examines the historical and potential land use change and GHG emissions associated with oil sands development in Canada. Disturbance occurred between 1985 and 2009 from oil sands development were identified using remote sensing technique and mapped onto spatially explicit soil, biomass and peatlands carbon maps. We found that land use and GHG disturbance of oil sands production, especially in-situ technology that will be the dominant technology of choice for future oil sands development, are greater than previously reported. We estimate additional 500 km^2 and 2,400 km^2 of boreal forest including carbon-rich peatlands would be disturbed from surface mining and in-situ production, respectively, between 2012 and 2030; releasing additional 107–182 million tonnes of GHG from land use alone. Future efforts to monitor land use impacts of in-situ production are needed to reduce landscape impacts and associated GHG emissions. In addition, land reclamation after oil sands projects needs to be enforced for broad ecological benefits together with GHG benefits.

1.   Introduction

Oil sands are naturally occurring mixtures of bitumen, sand and other mineral matter, and water. They are found in three main deposits in Alberta: the Athabasca, Cold Lake, and Peace River deposits. Bitumen can be surface mined when it is deposited at shallow depths of less than ~70 m. Deeper deposits are accessed through in-situ technologies, which most commonly inject steam underground to reduce bitumen viscosity. The Canadian Association of Petroleum Producers expects the oil sands industry will reach 1.8 billion barrels (4.9 mbd) by the end of 2030 (CAPP 2013b).

A large body of studies show that oil sands industries have large environmental impacts, including effects on climate, land, water, and air quality (Charpentier et al. 2011, Jordaan 2012, Jordaan, Keith, and Stelfox 2009, Sego 2008, Griffiths, Woynillowicz, and Taylor 2006, Woynillowicz, Severson-Baker, and Raynolds 2005, Rooney, Bayley, and Schindler 2012, Schneider and Dyer 2006, Kurek et al. 2013, Kelly et al. 2010, Kelly et al. 2009, Schindler 2014, Englander, Bharadwaj, and Brandt 2013, Brandt 2012, Yeh et al. 2010). Surface mining technology and in-situ technology have different environmental impacts (Jordaan, Keith, and Stelfox 2009, Woynillowicz, Severson-Baker, and Raynolds 2005, Schneider and Dyer 2006, Griffiths, Woynillowicz, and Taylor 2006, Yeh et al. 2010). Surface mining requires the clearing and excavation of large areas. Land disturbance includes the mine site itself, the storage of overburden (biomass, soils, and other earth materials), as well as the creation of tailing ponds and end pit lakes. In contrast, in-situ recovery requires infrastructure such as central processing facilities, networks of seismic lines, access roads, pipelines, and well pads. Previous studies examining the land use impacts of oil sands production focused on habitat loss, fragmentation, and other ecological effects (Jager, Carr, and Efroymson 2006, Jordaan, Keith, and Stelfox 2009, Lee and Boutin 2006, Rooney, Bayley, and Schindler 2012). A number of recent studies have begun to study the reclamation of disturbed oil sands areas in the post-mine landscape; particularly in relation to peatland ecosystems (Rowland et al. 2009, Price, McLaren, and Rudolph 2009) and their import role in landscape carbon (C) storage, biodiversity and habitat availability, and regulation of regional hydrology. However, oil sands land use disturbance, particularly GHG emissions, have not been examined in detail particularly the total historical and future impacts.

This study is the first comprehensive and spatially detailed land use impact study from oil sands production using state-of-the-art remote sensing and spatially explicit biomass, soil and peatlands carbon datasets. A total of 5 mining projects and 7 in situ projects were analyzed (Figure 1).
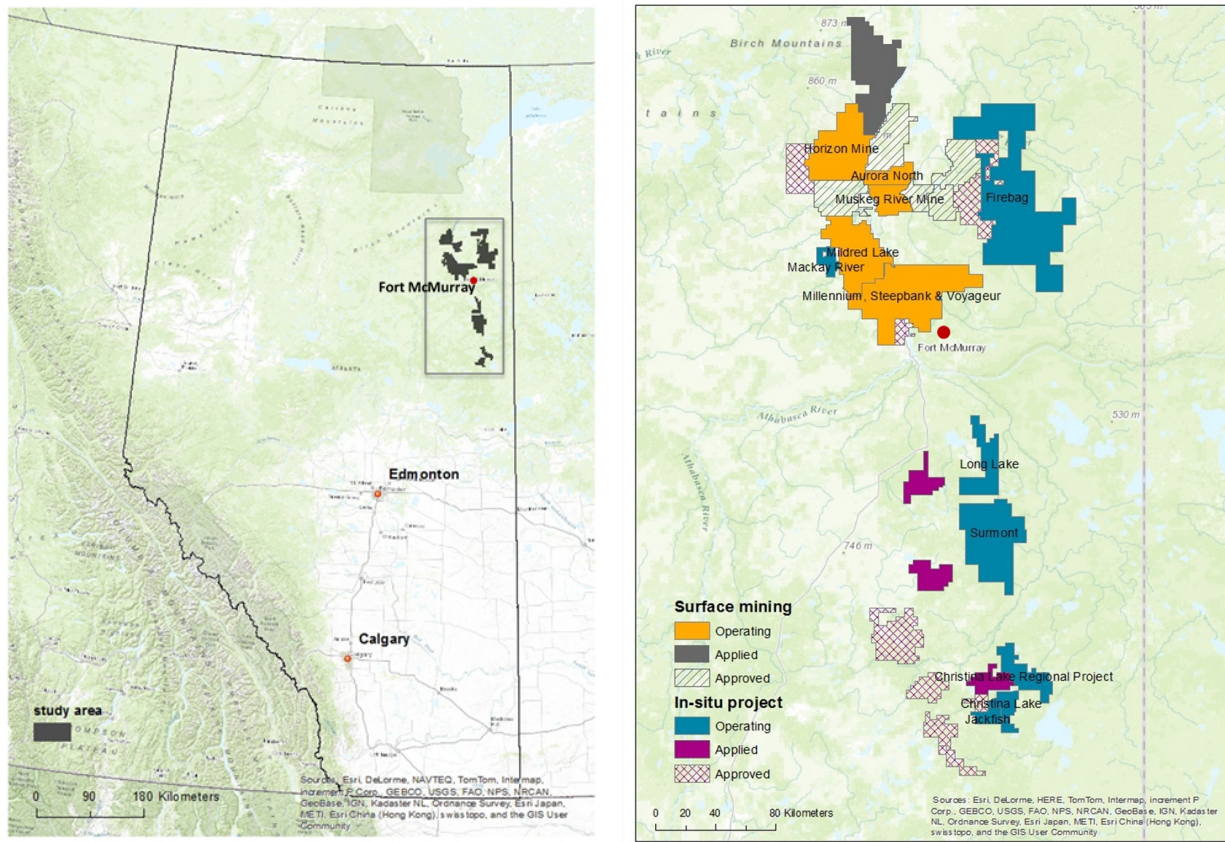

Figure 1. Left: Location of Study area in Alberta, Canada. Black color represents the study area. Right: Study area including 5 operating mines and 7 operating in-situ project sites. The colors represent the status of oil sands project in 2009. Orange areas represent active mines and blue areas represent active in-situ projects. Applied and approved sites are not relevant to our study but provide relevant information regarding relative locations of future disturbances. Source: Alberta Environment and Sustainable Resource Development (2011).

2.   Materials and Methods

We determine LUC associated with oil sands production using satellite remote sensing imagery between 1985 and 2009. The disturbed areas were mapped onto spatially explicit soil, biomass and peatland carbon maps. The carbon changes from soil C stock loss, biomass stock loss, foregone sequestration, and vegetation regrowth were calculated. These give us the project-specific LUC, land use intensity (LUI), carbon stock changes, and land use GHG intensity.

In general, oil sands developments tend to occur in phases. In some cases, large disturbances occur at the beginnings of a project due to land clearing and preparation, and infrastructure development. Energy production tends to be lower at the initial stage and increases slowly. Projects then gradually expand to new areas and abandon lands that no longer produce oil, which are required to be reclaimed later. We project future land use intensity and GHG intensity to the full lifetime of project based on projected future land use and GHG emissions, and the estimated ultimate recovery (EUR) of each project.

2.1 Land Classification: Remote Sensing

Satellite imagery from the Landsat 5 Thematic Mapper was acquired from the United States Geological Survey (USGS 2013) to map land cover change that has occurred in greater Athabasca oil sands region between 1985 and 2009. Six of these images (from Landsat's path 42 row 20) include coverage of the Lower Athabasca region, north of Fort Murray, Alberta, Canada, and were selected at approximately five-year intervals (September 28, 1985, June 11, 1992, September 24, 1995, June 15, 1999, June 28, 2004, and September 14, 2009). The other six images (path 41 row 21) include coverage south of Fort Murray, and were likewise selected at approximately five-year intervals (July 28, 1987, October 8, 1991, August 13, 1994, August 27, 1999, October 11, 2004, and September 23, 2009). Due to high inter-seasonal sun angle variability at this region's high latitude (approximately 57° N), and to minimize major phenological differences in vegetation that could confound change detection methods, the above image dates were selected based on the criteria that they were 1) cloud-free above the study sites and 2) collected during summer or early fall when seasonal conditions were most favorable for remote sensing detection. More detailed description of remote sensing techniques, land use classification method, and calibration can be found in the Supplementary Information (SI) Section S1.

2.2 Carbon Stock and Carbon Emissions

We rely on several sources to estimate biomass carbon values for the study region. Canada's National Forest Inventory (NFI) created a biomass data table and map that can be downloaded and opened in ArcGIS:

http://www.arcgis.com/home/item.html?id=07754b7affbf4322857acf984088898d (Last Modified on January 18, 2012). The resolution of the map is coarse. Nonetheless, it is the best open source data we could find. Regional scale estimates of carbon stock in west-central Alberta

boreal forest is estimated to have an average of 43 t C/ha (Banfield et al. 2002). Sampling of mature stand has higher biomass values of mean = 98 t C/ha, with a minimum of 21 t C/ha and a maximum of 199 t C/ha.

Soil carbon data in the study area is from The Soil Landscapes of Canada (SLC version 2). As one part of the National Soils Database, SLC version 2 was maintained by the Eastern Cereal and Oilseed Research Center of Agriculture and Agri-Food Canada. There are 46 polygons in our study area. Each of them is associated with total Soil C value and surface soil C value. For surface soil carbon, the values range from 0-212 t C/ha) and the weighted average is 108 t C/ha. For total soil carbon, the values range from 0-751 t C/ha) and the weighted average is 357 t C/ha (SI Section S2).

Oil sands production occurs primarily in wetland-rich area of boreal forest, peatland bogs, and peatland fens. Yet, high-quality direct measurement of peatland location and carbon content is not avaiable for our study area. Therefore, we estimate peatland C values based on the study by Beilman, Vitt et al. (2008). Beilman, Vitt et al. (2008) contains high-resolution wetland map data, available peat C characteristic and peat depth datasets, and geostatistics estimating the organic C stocks contained in peat for the wetland-rich boreal region of the Mackenzie River Basin, Alberta. A wetland inventory of both peatlands and nonpeat-accumulating wetlands was created for the study area from aerial photographs of 1: 15 000–1: 40 000 scale, and the classification of vegetation and physiography according to Halsey and Development (2003). Three generalized peatland types were considered: treed bogs, treed fens (wooded fens), and open fens (treeless, including both shrub- and sedge-dominated fens). We used spatially-explicit peatland datasets to estimate the percentage of peatlands in the disturbed areas of each site, and found that the range was 2-58% of the total disturbed areas (SI Section 2). In peat areas, wooded peatlands have the highest amount of biomass per unit area, followed by shrubby, and open fens. Of the wooded peatlands, bogs have the highest above-ground biomass (Vitt et al. 2000). Vitt, Hasley et al. (2000) estimated total above-ground biomass to be 3.875 t C/ha for wooded bogs and 1.27-1.375 t C/ha for wooded, shrubby, and open fens (using biomass to carbon factor of 0.5) for all continental western Canadian peatland sites. In Mackenzie River Basin (South of the surface mining areas), treed fen area is greatest (52% of total peatland area), followed by bog area (38%). For simplicity, we assume 3.875 t C/ha for peatlands biomass for all of the areas in

6

the study region. Overall, we assign the following total biomass values to the study regions: Coniferous Forest and Broadleaf Forest: 43 t C/ha; Bogs and Fens – non peatland: 35.5 t C/ha (= (4+67)/2); and Bogs and Fens – peatland: 3.875 t C/ha (Supplementary Information, SI, Section 2).

Soil carbon is typically reported for the top 30 cm (surface soil carbon) or to a depth of 100 cm (100 cm soil carbon). In disturbed areas, we assume that between 50-95% of the 100 cm soil C stock is lost in surface mining operations (Rooney, Bayley, and Schindler 2012); and 20-40% of the surface soil carbon is lost for in-situ operations (Wei et al. 2014). If a land is reclaimed according to our remote sensing analysis, we do not account for GHG losses from the initial land use. More detailed description of carbon loss and carbon emission calculations and equations can be found in SI Section S2.

2.3   Land Use Intensity and Carbon Intensity

Multiplying the observed LUI with the estimated carbon loss per unit disturbed area yields an estimate of the LUC carbon intensity (CI) for oil sands projects (Yeh et al. 2010). Future LUC impacts if the remaining established reserved were fully developed were estimated by extrapolating the land use impacts vs. *cumulative* production of a project lifetime.

The ERCB (2013) estimates the in-place volumes and established mineable and in situ crude bitumen reserves on both a project and deposit basis. The in-place volumes were determined using geophysical logs, core, and core analyses. Factors were then applied to the initial mineable volume in place to determine the established reserves. A series of reduction factors were applied to take into account inaccessible bitumen due to environmental protection corridors along major rivers, small isolated ore bodies, and the location of surface facilities (plant sites, tailings ponds, and waste dumps)(ERCB, 2013). A combined mining and extraction recovery factor of 82 percent is applied to this reduced resource volume. This recovery factor reflects the combined loss, on average, of 18 percent of the in-place volume by mining operations and extraction facilities. The resulting initial established reserves for surface mining project sites are shown in Table S1.

For the in-situ projects, data is taken from companies' Annual Information Forms that they are required to report each year. Similar to the initial mineable volume in place for the surface

mining projects, estimates were given as the original bitumen resources in place (OBIP), or producible oil in place (POIP), as indicators of resource volumes amenable to recovery. These annual reports also include detailed expected recovery factors for project sites by drainage area, pad, or by pattern and typically range from 40-70%. Table S1 summarizes the aggregated estimates for each project site based on the latest companies' Annual Information Forms.

Since project-level LUI shows a power-law relationship associated with economies of scale (shown in Section 3, Figures 4 and 5), we use the initial established reserves (IER) or estimated ultimate recovery (EUR) of crude bitumen and the fitted LUI curve to project future LUC and carbon emissions for the remaining lifetime of these projects. The equations and fitted regression lines are described in SI Section S3 and the results are shown in the next section

Once the potential LUC areas (million m^2) are known, we can estimate the total biomass and soil C emissions associated with converting these land. Since we do not know the exact locations of future land use, we use the average land use CI for each project to calculate the total C emissions associated with converting these areas for developing the remaining oil reserves (SI Equation 11). The carbon intensity of oil sands project for the entire project lifetime can thus be estimated based on the total *projected* carbon emissions from land use disturbance if the total projected energy is fully developed divided by the estimated total energy produced for a given project site (SI Equation 12).
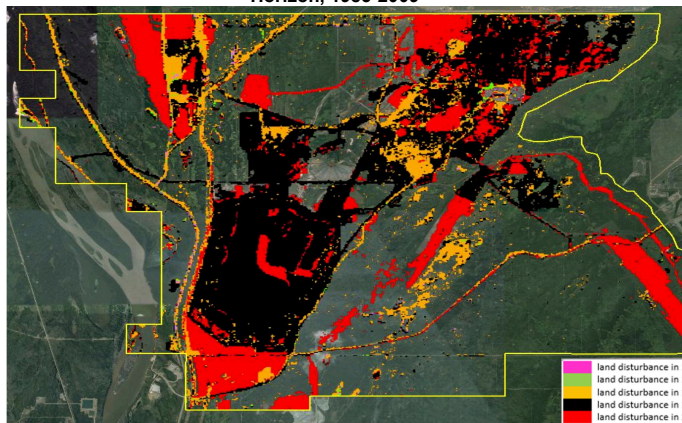
3.   Results

Figures 2 and 3 show the land use change results using true images overlaid by period of disturbance. The gross land use change showing disturbed areas in black and white are shown in Figures S1 and S2).
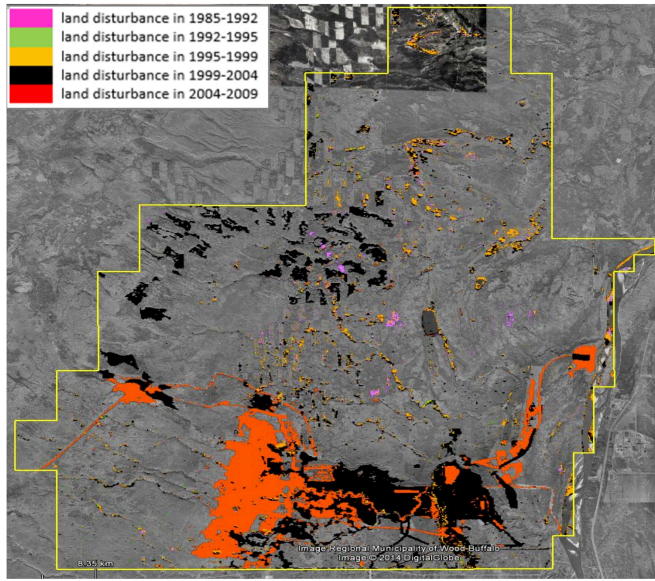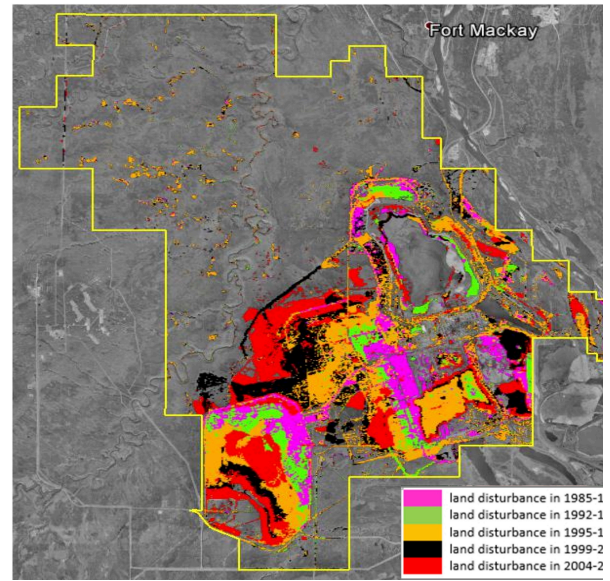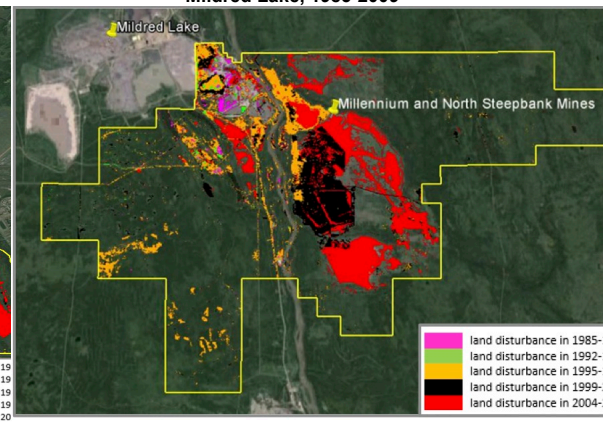
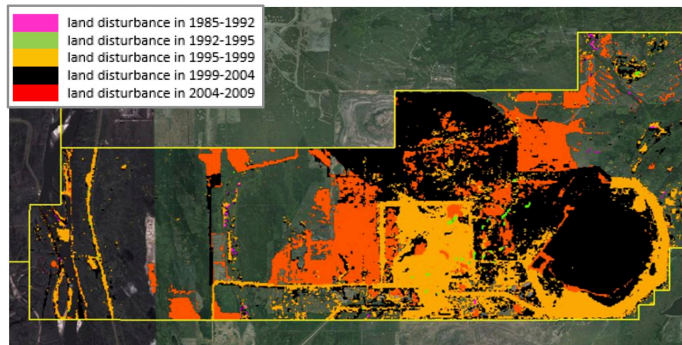**Figure 2.** Land use expansion of surface mining projects by period overlaid on 2013 map. The yellow boxes represent project boundaries.

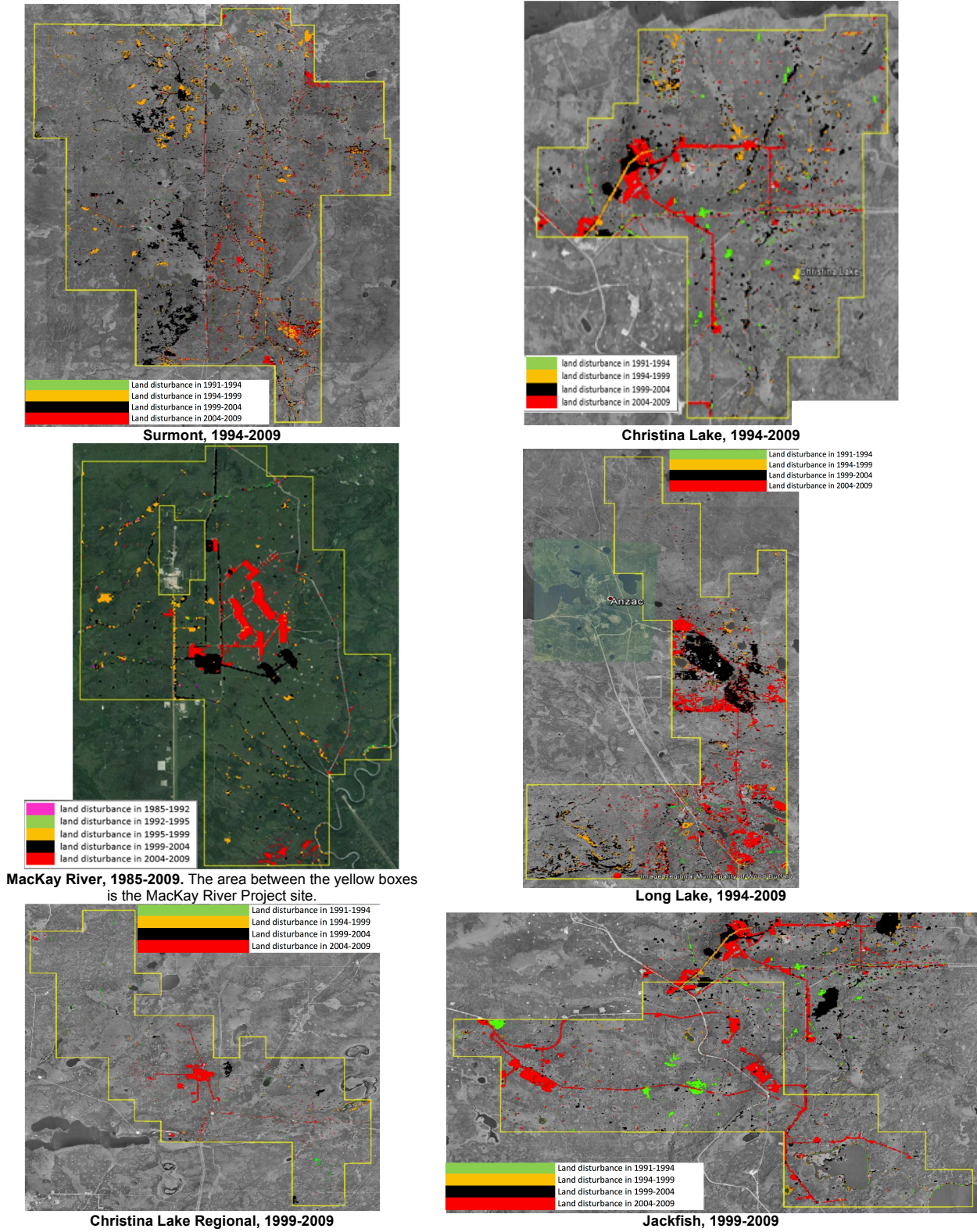**Figure 3.** Land use expansion of in-situ projects by period overlaid on 2013 map. The yellow boxes represent project boundaries.

The observed LUI for mining and in-situ projects are shown in Figure 4 by 5-year production volume and Figure 5 by cumulative production volume.

Figure 4. Net/gross land use intensity for mining (top) and in-situ (bottom) projects by 5-year production volume (1985-2009).
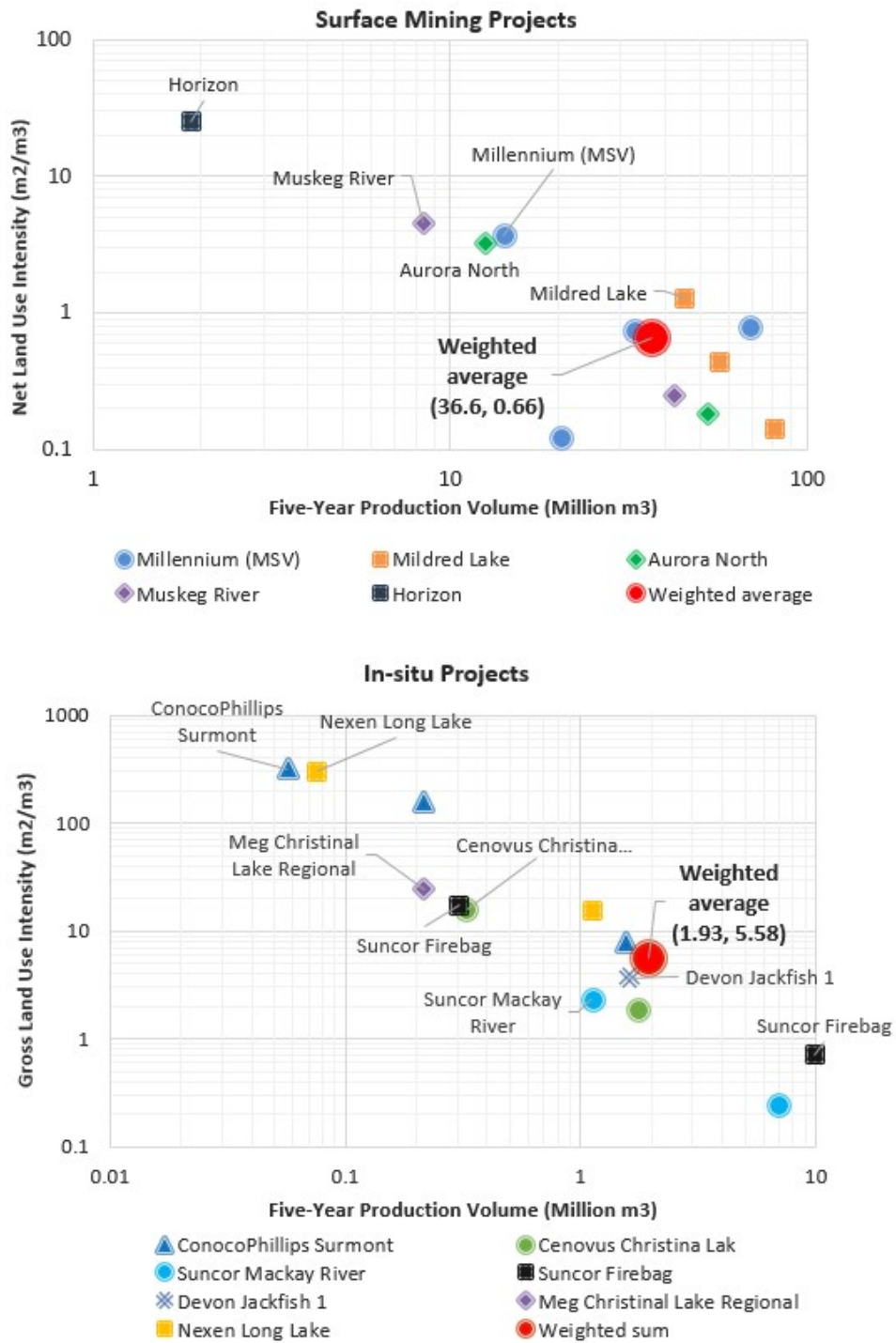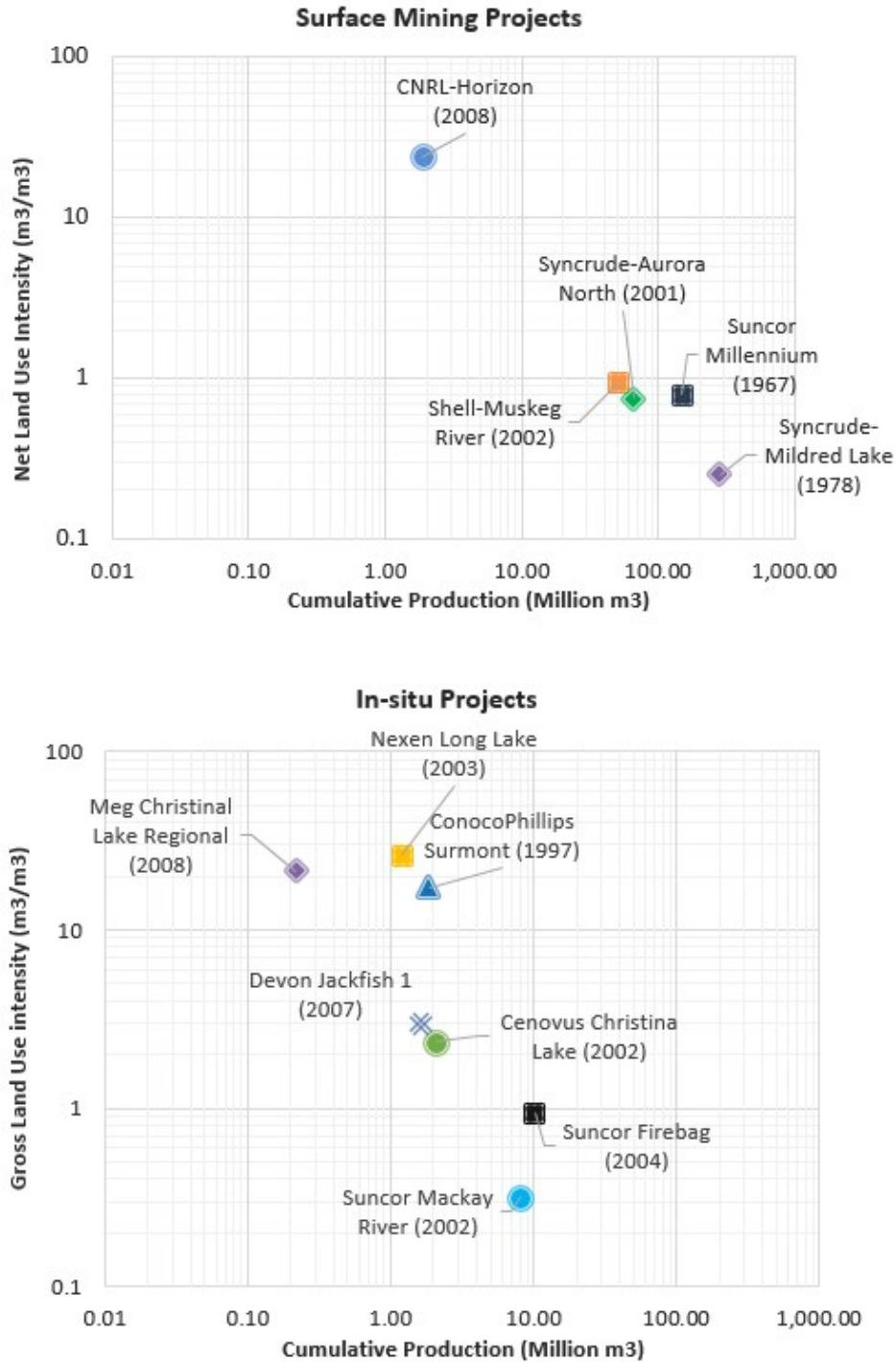
Figure 5. Net/gross land use intensity for mining (top) and in-situ (bottom) projects by cumulative production volume, 1985-2009.

Our analysis shows that land disturbed per m^3 of bitumen produced (m^2 land/m^3 bitumen) varies by a factor of 100 between projects and over time. Land use intensity (LUI) of surface mining

projects ranged from 0.25–24 m^2/m^3 for 1985-2009, and 0.31–26 m^2/m^3 for in-situ projects (Figures 4 and 5). For example, the CNRL-Horizon surface mining project, which began production in 2009, has the highest recent LUI (24 m^2/m^3) compared with other older mining projects. Its land use footprint is already equivalent to two other mining projects (Syncrude-Aurora North and Shell Muskeg River), or 44-48 million m^2, despite 50-65 times lower cumulative production volumes compared with the other two projects.

Contrary to the previous findings that land use intensity of in-situ projects are lower than surface mning (Jordaan, Keith, and Stelfox 2009), we found that in-situ projects have significantly higher weighted average LUI of 3.6 m^2/m^3 compared to 0.58 m^2/m^3 for surface mining (Figures 4 and 5). Three in-situ projects in the study area (ConocoPhillips Canada-Surmont, Nexen-Long Lake and MEG Energy Corp.-Christina Lake Regional), have the highest LUI observed. The reasons for this disturbance vary. Long Lake has a central processing facility (CPF) in the north, as well as significant disturbance (associated with seismic features, well activity and drainage areas) identified in the Kinosis SAGD area in the south between 2004 and 2009 (Nexen 2011). In contrast, Surmont site disturbance is caused largely not by its CPF but by the *extensiveness* of disturbance across the landscape in the form of road infrastructure, well pads, and the forest areas replaced by bare soil. These areas correlate closely with identifiable seismic features and drainage areas in the company's Annual Performance Review (ConocoPhilips 2013).

Both land use and production change over the life of a project. When land use intensity (LUI) is plotted against cumulative energy production for multiple surface mining and in-situ projects, the data show a power-law relationships associated with economies of scale and experience curves (Figure 6). Overall LUI of oil sands production decreases by 45% and 53% for surface mining and in-situ projects, respectively with each doubling of cumulative production. Although the surface mining curve lies at higher values than the in-situ curve for a given level of cumulative production, surface mining projects tend to have greater scale and thus have overall higher cumulative production and lower land use intensity compared with the in-situ projects studied.
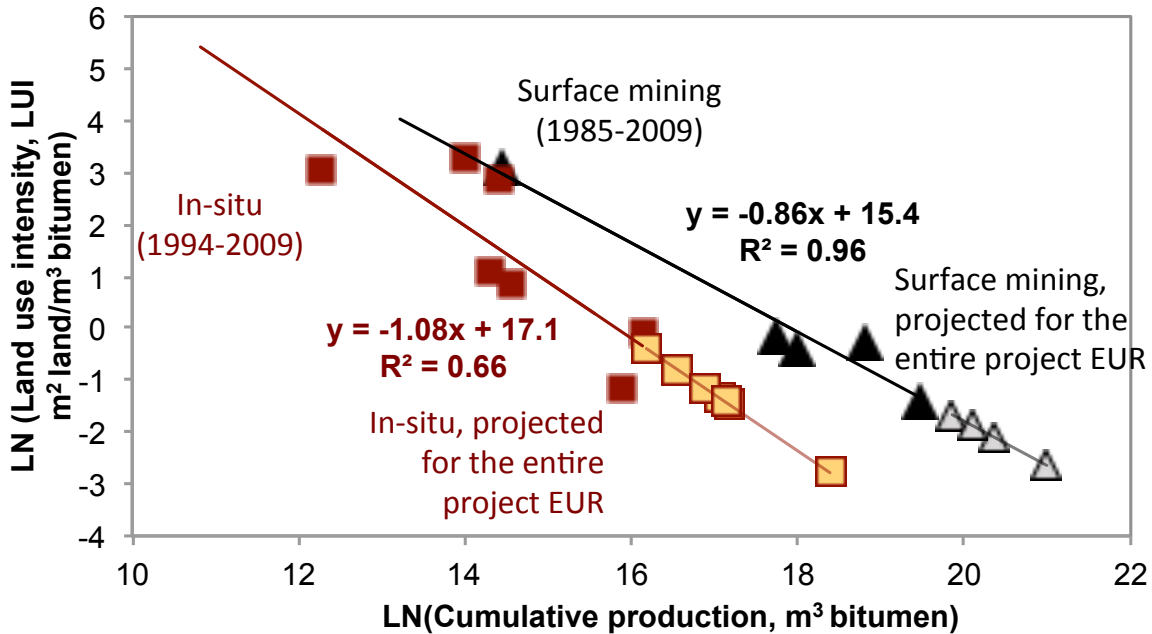
Figure 6. Observed land use intensity (LUI) (solid symbols) and cumulative bitumen production of mining (1985-2009, triangles) and in-situ (1994-2009, squares) projects plotted on a log-log scale. The areas underneath the regression lines represent the cumulative land use impacts of oil sands projects. Also plotted are the projected LUI (open symbols) based on estimated ultimate reserves (EUR) of each project and the cumulative land use impacts (represented by the areas underneath the regression line extending to the open symbols) over the entire lifetime of oil sands projects

We found that between 1985 and 2009, land use GHG emissions were around 2.2 – 4.0 gCO_2e/MJ of synthetic crude oil (SCO) and bitumen mixture produced for surface mining and 1.8 – 2.8 gCO_2e/MJ of bitumen produced for in-situ production. Total CO_2e emissions from land use disturbance for the five surface mining and seven in-situ projects were estimated at 12.6 – 22.7 million tonnes C lost through 2009 (Table 1).

Table 1. Estimated potential LUC areas (million m^2)(top table) and carbon emissions (bottom table) if the remaining mining and in-situ reserves were to fully developed

Site	EUR (million m³)	Cumulative Production up to 2009 (million m³)	Total area change up to 2009 (million m²)	Net/Gross Intensity up to 2009 (m²/m³)	Estimated cumulative LUC over the entire project lifetime (million m²)	Estimated average LUI over the entire project lifetime (m²/m³)
Surface mining						
MSV mines	687	149	117	0.78	232	0.34
Syncrude (Mildred Lake and Aurora North)	1306	348	116	0.33	227	0.17
Muskeg and expansion	419	50.8	43.9	0.86	187	0.45
Horizon	537	1.88	41.5	22.09	358	0.67
Sum/avg.	2949	550	317.4	*0.58*	1,004	0.34
In-situ						
Surmont	15.2	1.84	31.9	17.4	47	3.12
Christina Lake	25.8	2.07	4.86	2.3	23	0.90
Mackay River	21.9	8.04	2.53	0.3	10	0.44
Long Lake	28.5	1.21	31.5	26.1	55	1.94
Firebag	96.5	10.1	9.50	0.9	24	0.25
Jackfish	27.4	1.63	4.85	3.0	25	0.92
Christina Lake Regional	10.6	0.216	4.61	21.3	37	3.52
Sum/avg.	226	25.1	89.7	*3.57*	222	0.98

	Total C emissions to date, 2009 (Mt C)		Average Land use CI (tC/ha)		Estimated total C emissions from the entire lifetime of the project (Mt C)		Estimated LU CI from the entire lifetime of the project (gCO₂e/MJ)	
Surface mining								
	Low	High	Low	High	Low	High	Low	High
Suncor-MSV mines	8.7	8.8	698	706	16.4	16.6	2.42	2.45
Syncrude (Mildred Lake and Aurora North)	6.5	6.6	453	461	10.5	10.7	0.80	0.82
Mildred Lake	3.0	3.1	318	327	-	-		
Aurora North Mine	3.5	3.5	704	711	-	-		
Muskeg and expansion	3.5	3.5	719	727	13.7	13.8	2.98	3.01
Horizon	1.9	2.0	411	419	15.2	15.5	2.87	2.92
Total	*20.6*	*20.9*	*515*	*523*	55.8	56.6	1.87	1.90
In-situ								
Surmont	0.18	0.28	55	88	0.26	0.41	1.57	2.49
Christina Lake	33	55	68	114	0.16	0.27	0.56	0.94
Mackay River	13	19	52	74	0.05	0.07	0.21	0.30
Long Lake	147	225	47	71	0.26	0.39	0.82	1.26
Firebag	56	88	56	89	0.14	0.21	0.13	0.20
Jackfish	34	57	71	118	0.18	0.30	0.60	0.99
Christina Lake Regional	30	49	66	105	0.25	0.39	2.12	3.39
Total	*0.49*	*0.77*	*57*	*87*	*1.3*	*2.1*	*0.56*	*0.89*

We estimate that if the remaining IER/EUR of existing projects were fully developed (representing a total of 20 billion bbl production, of which 93% is from surface mining development), the total land use disturbance will be ~1000 km² for the five surface mining projects and ~220 km² for the seven in-situ sites, with an average CI over the life of the projects of 1.1 – 1.9 gCO₂e/MJ for surface mining and 0.56 –0.89 gCO₂e/MJ for in-situ production. The results for the projected potential LUC areas and total GHG emissions are shown in Table 1, respectively.

Given the projected oil sands production forecast to 2030 (CAPP 2013a), an additional 9.2 and 15 billion bbl of oil sands will be produced from surface mining and in-situ production, respectively. Using the same emission factors estimated in this study, an additional 58-105 and 49–77 million tonnes CO_2e are expected to be emitted from LUC due to surface mining and in-situ production, respectively, between 2012-2030. The total net land use disturbance may exceed 500 km^2 and 2,400 km^2 of boreal forest including peatlands from surface mining and in-situ production, respectively.

4.   Discussion

Oil sands production occurs primarily in regions of boreal forest that often have abundant wetlands and carbon-rich peatlands (Turetsky et al. 2002). LUC includes conversions of mixed forest/peatlands, coniferous forests, and broadleaf forests to bare soil and water, and conversion of bare soil to water. Carbon emissions associated with LUC from oil sands development include clearing of vegetation and trees, loss of soil carbon, foregone sequestration, and re-sequestration due to vegetation regrowth as a result of reclamation or natural vegetation regrowth. Once a forest is cleared, it no longer sequesters carbon (thus the "foregone sequestration" had the forest not been disturbed) until it is reclaimed back to forest to resequester carbon again.

The largest uncertainties in this study are soil carbon loss factors. Soil carbon content is measured at various depths and reported as such in this study: 0–30 cm, and up to 100 cm soil carbon. More thorough empirical studies and approaches to estimate the soil carbon that is oxidized due to different types of disturbance (e.g. mining activities vs. building access roads vs. constructing well pads) would greatly improve our understanding of land use GHG emissions. While LUI is higher for in-situ projects than for mining projects, the CI from land disturbance of in-situ projects is lower due to the assumed lower soil C losses. If the soil C loss factors are higher than we assume here, or the depth of soil affected is greater than 30 cm for in-situ projects, then the total carbon emissions associated with in-situ projects will be greater than estimated.

Our observed LUI of in-situ projects 1987-2009 are orders of magnitude higher than the only published study, Jordaan et al. (Jordaan, Keith, and Stelfox 2009)(0.31 – 26 m^2/m^3 vs. 0.11

m^2/m^3, respectively), which used computer simulation estimates based on best practices. The estimated lifetime LUI of in-situ projects are lower than observed LUI of in-situ projects 1987-2009, but still significantly higher than the previous estimates by Jordaan et al. We suspect that this may be due to the fact that actual operations may differ from computer simulation-based estimates for a given location due to variations in geology and local conditions. In addition, some of the land use disturbance such as forest clearing and drainage areas that are observable in satellite images were not included in the estimates in Jordaan et al (2009).

Our analysis found a large degree of variation in land use practices among projects, particular for in-situ production. Understanding the drivers of this variation in LUC and LUI could suggest more effective means to reduce the environmental impact of oil sands production. Future work is needed to carefully monitor the land use impacts of in-situ production and develop best practices to reduce their impacts on the landscape. The massive land disturbance as we and others concluded from oil sands operation also reiterates the importance of enforcing land reclamation after oil sands projects as companies and Alberta government agreed for broad ecological benefits together with GHG benefits.

References

Banfield, G. E., J. S. Bhatti, H. Jiang, and M. J. Apps. 2002. "Variability in regional scale estimates of carbon stocks in boreal forest ecosystems: results from West-Central Alberta." *Forest Ecology and Management* 169 (1–2):15-27. doi: http://dx.doi.org/10.1016/S0378-1127(02)00292-X.

Brandt, A.R. 2012. "Variability and uncertainty in life cycle assessment models for greenhouse gas emissions from canadian oil sands production." *Environmental Science & Technology* 46 (2):1253-1261.

CAPP. 2013a. Crude Oil: Forecast, Markets & Transportation. Canadian Association of Petroleum Producers.

CAPP. 2013b. Crude Oil: Forecast, Markets and Transportation. Canadian Association of Petroleum Producers
.

Charpentier, Alex D., Oyeshola Kofoworola, Joule A. Bergerson, and Heather L. MacLean. 2011. "Life cycle greenhouse gas emissions of current oil sands technologies: GHOST model development and illustrative application." *Environmental Science & Technology* 45:9393–9404. doi: dx.doi.org/10.1021/es103912m.

ConocoPhilips. 2013. Annual Surmont SAGD Performance Review Approvals 9460, 9426 and 11596 Subsurface.

Englander, Jacob G, Sharad Bharadwaj, and Adam R Brandt. 2013. "Historical trends in greenhouse gas emissions of the Alberta oil sands (1970–2010)." *Environmental Research Letters* 8 (4):044036.

Griffiths, Mary, Dan Woynillowicz, and Amy Taylor. 2006. Troubled Waters, Troubling Trends: Technology and Policy Options to Reduce Water Use in Oil and Oil Sands Development in Alberta.

Jager, Henriette I., Eric A. Carr, and Rebecca A. Efroymson. 2006. "Simulated effects of habitat loss and fragmentation on a solitary mustelid predator." *Ecological Modelling* 191 (3-4):416-430.

Jordaan, Sarah M. 2012. "Land and Water Impacts of Oil Sands Production in Alberta." *Environmental Science & Technology* 46 (7):3611-3617. doi: 10.1021/es203682m.

Jordaan, Sarah M., David W. Keith, and Brad Stelfox. 2009. "Quantifying land use of oil sands production: a life cycle perspective." *Environmental Research Letters* 4 (2):024004.

Kelly, Erin N., David W. Schindler, Peter V. Hodson, Jeffrey W. Short, Roseanna Radmanovich, and Charlene C. Nielsen. 2010. "Oil sands development contributes elements toxic at low concentrations to the Athabasca River and its tributaries." *Proceedings of the National Academy of Sciences* 107 (37):16178-16183. doi: 10.1073/pnas.1008754107.

Kelly, Erin N., Jeffrey W. Short, David W. Schindler, Peter V. Hodson, Mingsheng Ma, Alvin K. Kwan, and Barbra L. Fortin. 2009. "Oil sands development contributes polycyclic aromatic compounds to the Athabasca River and its tributaries." *Proceedings of the National Academy of Sciences* 106 (52):22346-22351. doi: 10.1073/pnas.0912050106.

Kurek, Joshua, Jane L. Kirk, Derek C. G. Muir, Xiaowa Wang, Marlene S. Evans, and John P. Smol. 2013. "Legacy of a half century of Athabasca oil sands development recorded by lake ecosystems." *Proceedings of the National Academy of Sciences* 110 (5):1761-1766. doi: 10.1073/pnas.1217675110.

Lee, Philip, and Stan Boutin. 2006. "Persistence and developmental transition of wide seismic lines in the western Boreal Plains of Canada." *Journal of Environmental Management* 78 (3):240-250.

Nexen. 2011. Long Lake 2010-Subsurface performance presenation.

Price, Jonathan S., Robert G. McLaren, and David L. Rudolph. 2009. "Landscape restoration after oil sands mining: conceptual design and hydrological modelling for fen reconstruction." *International Journal of Mining, Reclamation and Environment* 24 (2):109-123. doi: 10.1080/17480930902955724.

Rooney, Rebecca C., Suzanne E. Bayley, and David W. Schindler. 2012. "Oil sands mining and reclamation cause massive loss of peatland and stored carbon." *Proceedings of the National Academy of Sciences* 109 (13):4933-4937. doi: 10.1073/pnas.1117693108.

Rowland, S. M., C. E. Prescott, S. J. Grayston, S. A. Quideau, and G. E. Bradfield. 2009. "Recreating a Functioning Forest Soil in Reclaimed Oil Sands in Northern Alberta: An Approach for Measuring Success in Ecological Restoration All rights reserved. No part of this periodical may be reproduced or transmitted in any form or by any means, electronic or mechanical, including photocopying, recording, or any information storage and retrieval system, without permission in writing from the publisher." *J. Environ. Qual.* 38 (4):1580-1590. doi: 10.2134/jeq2008.0317.

Schindler, David W. 2014. "Unravelling the complexity of pollution by the oil sands industry." *Proceedings of the National Academy of Sciences* 111 (9):3209-3210. doi: 10.1073/pnas.1400511111.

Schneider, Richard R., and Simon Dyer. 2006. Death by a Thousand Cuts: The Impacts of In Situ Oil Sands Development on Alberta's Boreal Forest. The Pembina Institute.

Sego, David. 2008. "Environmental impact of the oil sands development." 2008 Gussow-Nuna Geoscience Conference.

Turetsky, Merritt, Kelman Wieder, Linda Halsey, and Dale Vitt. 2002. "Current disturbance and the diminishing peatland carbon sink." *Geophys. Res. Lett.* 29 (11):1526, doi:10.1029/2001GL014000.

USGS. 2013. USGS Global Visualization Viewer.

Vitt, D. H., L. A. Halsey, I. E. Bauer, and C. Campbell. 2000. "Spatial and temporal trends in carbon storage of peatlands of continental western Canada through the Holocene." *Can. J. Earth Sci.* 37:683-693.

Wei, Xiaorong, Mingan Shao, William Gale, and Linhai Li. 2014. "Global pattern of soil carbon losses due to the conversion of forests to agricultural land." *Scientific Reports* 4:4062. doi: 10.1038/srep04062.

Woynillowicz, Dan, Chris Severson-Baker, and Marlo Raynolds. 2005. Oil Sands Fever: The Environmental Implications of Canada's Oil Sands Rush. The Pembina Institute.

Yeh, Sonia, Sarah M. Jordaan, Adam R. Brandt, Merritt R. Turetsky, Sabrina Spatari, and David W. Keith. 2010. "Land use greenhouse gas emissions from conventional oil production and oil sands." *Environmental Science & Technology* 44:8766-8772. doi: 10.1021/es1013278.

Supplementary Information

Past and Future Land Use Impacts of Canadian Oil Sands and Greenhouse Gas Emissions

S. Yeh[a], A. Zhao[a], S. Hogan[b], A.R. Brandt[c], J.G. Englander[c], D.W. Beilman[d], M.Q. Wang[e]

[a] Institute of Transportation Studies, University of California, Davis, CA USA 95060.

[b] Geography Graduate Group, University of California, Davis, CA USA 95060.

[c] Department of Energy Resources Engineering, Stanford University, Stanford, CA USA 94305-2220.

[d] Department of Geography, University of Hawaii at Mānoa, Honolulu, HI, USA 96822.

[e] Systems Assessment Group, Energy Systems Division, Argonne National Laboratory, Lemont, IL 60439.

Corresponding author: Sonia Yeh, Institute of Transportation Studies, 1605 Tilia Street, University of California, Davis, CA USA 95060. Tel: (530) 830 2544; Email: slyeh@ucdavis.edu

1. Land Use and Land Cover Change Detection

1.1 Land Classification: Remote Sensing

Satellite imagery from the Landsat 5 Thematic Mapper was acquired from the United States Geological Survey (*1*) to map land cover change that has occurred in greater Athabasca oil sands region between 1985 and 2009. Six of these images (from Landsat's path 42 row 20) include coverage of the Lower Athabasca region, north of Fort Murray, Alberta, Canada, and were selected at approximately five-year intervals (September 28, 1985, June 11, 1992, September 24, 1995, June 15, 1999, June 28, 2004, and September 14, 2009). The other six images (path 41 row 21) include coverage south of Fort Murray, and were likewise selected at approximately five-year intervals (July 28, 1987, October 8, 1991, August 13, 1994, August 27, 1999, October 11, 2004, and September 23, 2009). Due to high inter-seasonal sun angle variability at this region's high latitude (approximately 57° N), and to minimize major phenological differences in vegetation that could confound change detection methods, the above image dates were selected based on the criteria that they were 1) cloud-free above the study sites and 2) collected during summer or early fall when seasonal conditions were most favorable for remote sensing detection.

The Landsat images were atmospherically corrected to represent surface reflectance using ATCOR 3 IDL software, in order to take full advantage of the images' spectral measurements and to partly normalize the images for change detection processing. This process was conducted because reflectance data, consisting of a ratio of incident sun radiation on a surface relative to its

exiting/reflected radiation, is commonly recognized as an optimal type of data for land cover monitoring. The calibration process exploited digital elevation model (DEM) data derived from the ASTER satellite system (also acquired from the USGS 2013) to optimize the calibrations by correcting for differences in albedo related to slope and aspect, and atmospheric density related to elevation. Canty's Multivariate Alteration Detection (iMAD) and Canonical Correlation for image normalization (*2*) was then used to cross-calibrate the Landsat reflectance images (matching reflectance levels of invariant targets in the images), to further improve confidence in eventual change detection analyses.

IsoData and K-Means classifications, which don't require user inputs to train their classification processes, were conducted upon several of the Landsat images to identify natural spectral breaks in land cover class separability. This technique is similar to research conducted by Gillanders, Coops et al. on the use of Landsat for monitoring the Athabasca oil sand region (*3*). The Landsat images, rendered in both true color and in color infrared, were then compared to the IsoData and K-Means classifications, using spectral signatures from the Landsat images that corresponded to the matching locations within the K-Means and IsoData classified images. The Landsat images where then compared with Google Earth's high spatial resolution 2013 DigitalGlobe imagery, land cover data from the Alberta Biodiversity Monitoring Institute (ABMI 2013), and wetland map and field data from Vitt, Halsey et al. (*4*) and Beilman, Vitt et al. (*5*), to establish ideal spectral signatures for soil, water, shrubs, mixed forest/peatlands, coniferous forest, and broad leaf forest, which were recognized as the predominate land cover types within this study's regions of interest.

111 Regions of interest (ROIs) for Landsat path-row 42-20 (including 6352 pixels), and 338 ROIs for path-row 41-21 (including 15,238 pixels) that together best represented the six land cover types, while capturing the spectral variability of the classes, were delineated within the Landsat images to train more robust supervised classifications in the future. These ROIs were overlaid on each of the Landsat images/dates, taking great care to ensure that the ROIs captured the same types of land cover in all of the Landsat image dates. This was necessary to ensure that subsequent supervised classifications would be comparable between years. Previous atmospheric calibrations and inter-annual cross calibrations also helped to ensure the classifications would be as comparable as possible. However, some unavoidable natural seasonal phenological and inter-annual variability in the vitality/appearance of vegetation inevitably introduced some variability between classifications.

The land cover ROIs identified within the Landsat imagery were again spatially cross referenced with Google Earth's 2013 DigitalGlobe imagery, land cover data provided by the Alberta Biodiversity Monitoring Institute (ABMI, 2013), and wetland data from Vitt, Halsey et al. (*4*) and Beilman, Vitt et al. (*5*), to verify that the ROI's did indeed represent the six target land cover classes of interest. The ABMI land class 'shrubs' was a small and intermittent component of the data north of Ft. McMurray (consisting of approximately <10% of ABMI's classifications for the operational sites, and exhibiting their lowest level of classification accuracy; with a 37.27% producer accuracy and 33.9% user accuracy). To simplify this questionable portion of the dataset, this class was not included in future Landsat pat 42 row 20 classifications.

Supervised classifications of all 12 Landsat images were then conducted using the machine learning classifier, Random Forests (RF), trained by the above ROIs. The 12 RF classified

images (two sets of six images) were clipped to only include the spatial extents of the oil sand operational sites (GIS data provided by Oil Sands Information Portal, Alberta Environment and Sustainable Resource Development). Change detection analyses of the RF classifications were then conducted separately on each of these sites (including 7 in-situ operations and 5 pit mining operations), divided into ten increments of time (North of Fort Murray/South of Fort Murray: 1985/1987 to 1992/1991, 1992/1991 to 1995/1994, 1995/1994 to 1999/1999, 1999/1999 to 1995/1994, 1995/1994 to 2009/2009, 1985/1987 to 2009/2009, 1992/1991 to 1999/1999, 1992/1991 to 2009/2009, 1995/1994 to 2009/2009, and 1999/1999 to 2009/2009). These analyses yielded map files (shapefiles) delineating changes from each type of land cover to each of the other types of land cover.

Because peatlands were difficult to classify and differentiate from other land cover types reliably with the Landsat data, Vitt, Halsey, et al.'s (*4*) percent peatland values were appended to the change detection results (shapefile attributes), so that the area of peatland disturbance could be estimated along with conversions of vegetated land cover to bare earth and water (as a % of the areas that were disturbed). Likewise, geospatial soil carbon data from The Soil Landscapes of Canada (SLC v. 2.2 1996 (*6*)) was appended to the change detection results to better estimate changes in belowground carbon values with changes in land cover.

1.2 Land Use Change

Geospatial project-specific gross LUC (m^2 or ha) for each time period (1985-1992, 1992-1995, 1995-1999, 1999-2004 and 2004-2009) is captured by the following equation:

LUC (gross) = conversion of Peatlands to Soil + conversion of Peatlands to Water + conversion of Broadleaf Forest to Soil + conversion of Broadleaf Forest to Water + conversion of Coniferous Forest to Soil + conversion of Coniferous Forest to Water + conversion of Soil to Water
(Equation 1)

Project-specific land reversion to forest or other vegetation (m^2 or ha) for each time period is captured by the following equation:

REVERSION = conversion of Soil to Peatlands + conversion of Soil to Broadleaf Forest + conversion of Soil to Coniferous Forest + conversion of Water to Peatlands + conversion of Water to Broadleaf Forest + conversion of Water to Coniferous Forest
(Equation 2)

Project-specific net LUC (m^2 or ha) is captured by the following equation:

LUC (net) = LUC (gross) – REVERSION   *(Equation 3)*

1.3 Land Use Intensity, LUI (m^2/m^3)

The geospatial land use disturbance data is combined with project-specific oil sands production volumes (Section 3.2) to obtain project-specific land use intensity (m^2/m^3).
The gross land use intensity for each time period can be calculated as:

$$LUI_{gross, i} = LUC \ (gross)_i \ / \ P_i \qquad \textit{(Equation 4)}$$

Where P_i is the total energy delivered (bitumen and/or SCO) (m^3) during time period i.
The net land use intensity can be calculated as:

$$LUI_{net, i} = LUC \ (net)_i \ / \ P_i \qquad \textit{(Equation 5)}$$

We first estimate the total energy delivered P_i given LUC_i (LUC (gross)$_i$ or LUC (net)$_i$) based on what we observed 1985-2009 (**historically observed LUI**) by calculating the observed land use disturbance between the period of observation (t = 0 to t = i) to energy produced/delivered during the same time period for a given project site.

We also make an effort to estimate the overall LUI for each project if the recoverable resources of each project were fully develop (**estimated lifetime LUI**). We do so by allocating all land use disturbance between the period of observation (t = 0 and t = i) and *future* expected land use disturbance to *total projected* energy produced for a given project site.

The later approach requires additional information for a given project:

- future energy production over the lifetime of a project;
- future rate of land use expansion and the location of future expansion;
- future foregone sequestration due to LUC;
- future biomass reversion from disturbed sites within the time period of concern;
- for surface mining, future emissions from tailings pond (considered in this study, calculated separately in the companion report (*7*)).

2. Carbon Stock, Carbon and Methane Emissions

Carbon stocks are affected by LUC through a variety mechanisms (*8*). The mechanisms we examined here include clearing of vegetation and trees, loss of soil carbon, foregone sequestration, and re-sequestration due to vegetation regrowth as a result of reclamation or natural vegetation regrowth. We do not include reported methane emissions from fine tailings as they not part of the land use emissions.

The carbon emissions associated with LUC from oil sands development is separated into two parts: biomass carbon emissions (ΔBio), and soil carbon emission (ΔSoil). Biomass carbon emissions (ΔBio) include biomass carbon loss due to conversion, foregone sequestration, and biomass carbon gains due to reversion:

$$\Delta\text{Bio} = \sum_i \sum_j (LUC(gross)_{i,j} \times BioC_j \times F_{bio} + LUC(gross)_{i,j} \times Seq_j \times T + REVERSION_{i,j} \times BioC_k) \qquad \textit{(Equation 6)}$$

where

LUC (gross)$_{I,j}$ is the project-specific gross LUC (ha) during time period i of vegetation type j,
$BioC_j$ is the biomass carbon stock (t C/ha) of pre-conversion land type j,
F_{bio} is the faction of biomass carbon loss after conversion,
Seq_j is the foregone sequestration rate (t C/ha/yr) of pre-conversion land type j,
T is the number of years that we account for the foregone sequestration,
$REVERSION_{i,j}$ is the observed areas revert back to forest (ha) during time period i of vegetation type j,
$BioC_k$ is the biomass carbon stock (t C/ha) of post-conversion land type k,
i is the study period, which includes 1985-1992, 1992-1995, 1995-1999, 1999-2004, 2004-2009.

$$\Delta\text{Soil} = \sum_j (LUC(gross)_{1985-2009,j} \times SoilC_j \times F_{soil}) \qquad \textit{(Equation 7)}$$

where

$LUC(gross)_{1985\text{-}2009,j}$ is the gross LUC (ha) of pre-conversion land type j between 1985-2009,
$SoilC_j$ is the soil carbon stock (t C/ha) of pre-conversion land type j,
F_{soil} is the faction of soil carbon loss after conversion,

$$\text{Total C loss} = \Delta\text{Bio} + \Delta\text{Soil} \qquad \textit{(Equation 8)}$$

2.1 Biomass Carbon Values for Boreal Forest and Wetland (BioC$_j$)

We rely on several sources to estimate biomass carbon values for the study region. Canada's National Forest Inventory (NFI) includes a biomass data table and map: http://www.arcgis.com/home/item.html?id=07754b7affbf4322857acf984088898d (Last Modified on January 18, 2012). For the whole of Alberta, the NFI has five biomass carbon categories (tonnes/ha): 0-25, 25-50, 50-100, 100-150, and >150. In the Athabasca oil sands region there are two biomass C categories: 25-50 and 50-100 tonnes/ha. Regional scale estimates of tree biomass carbon stocks in west-central Alberta boreal forest is estimated to have an average of 43 t C/ha (*9*). Mature stands have higher mean biomass values of 98 t C/ha, with a range of 21-199 t C/ha.

In peatlands it is typically the case that aboveground biomass and belowground living root biomass can be an order of magnitude smaller than in upland forests (*5, 10*). Our land cover classification "mixed forest/peatlands" include a mix of wetland and peatlands. For example, Bhatti, Errington et al. (*10*) sampled two study areas in boreal central Saskatchewan, approximately 600 km southeast of our study area, that include a mixture of upland forests and peatlands. The total stored carbon (including above-ground tree biomass, above-ground

understory biomass, and root biomass) had a range of 4-67 t C/ha (4-30 t C/ha in one site and 7-67 t C/ha in another) with the lower carbon stocks toward the peatland end of the ecotone.

Aboveground carbon varies across peatland types. Wooded peatlands have the highest amount of biomass per unit area, followed by shrubby, and open peatlands. Of the wooded peatlands, bogs (rainwater-fed peatlands) generally have the highest above-ground biomass (*11*). Vitt, Hasley et al. (*11*) estimated total above-ground biomass carbon to be 3.875 t C/ha for wooded bogs and 1.27-1.375 t C/ha for wooded, shrubby, and open fens (using biomass to carbon factor of 0.5) for all continental western Canadian peatland sites. In a nearby region of the southernmost Mackenzie River Basin (south of the surface mining areas), treed fen area is greatest (52% of total peatland area), followed by bog area (38%; Beilman, Vitt et al. (*5*). In Vitt, Hasley et al. (*11*) Table 4, there are n=8 pooled values that range from 99-887 g biomass m^{-2} and yield an average of 454.25. Thus, mean aboveground carbon would be 2.271 t C/ha. For simplicity, we conservatively assume 2.271 t C/ha for peatlands biomass carbon for all of the areas in the study region.

Overall, we assign the following total biomass values to the study regions: Coniferous Forest and Broadleaf Forest: 43 t C/ha; Mixed forest – non peatland: 35.5 t C/ha (= (4+67)/2); and Mixed forest – peatland: 2.271 t C/ha.

2.2   *Forest Soil Carbon (SoilC$_j$)*

Soil carbon data in the study area is from The Soil Landscapes of Canada (SLC v. 2.2). As one part of the National Soils Database, SLC 2.2 is maintained by the Eastern Cereal and Oilseed Research Center of Agriculture and Agri-Food Canada. The 1:1 million dataset was prepared in 1996 and revised in 1999. Based on correspondence with the experts from the Canada national soil database, there was no update since 1999. Other recent energy and resource studies utilize this dataset (*12*).

The SLC (version 2) database has one polygon shapefile and two attribute tables: the Carbon Polygon Attribute Table (CARBON.PAT) and the Carbon Component Table (CARBON.CMP). These attribute tables provided a variety of variables-some of which are used to calculate the soil carbon. A weighted average carbon content for each polygon was determined by the following formula:

$$\text{Carbon Content (kg/m}^2)$$
$$= \text{Thick (cm) x Bulk Density (g/m}^3) \text{ x Organic Carbon (\%) / 10} \textit{ (Equation 9)}$$

Forest soil carbon estimates were made for 2 depths due to the uncertainty of potential emissions associated with each depth. Surface carbon is summed for the top 30 cm while 100 cm carbon content is calculated to the depth of soil up to 100 cm.

There are 46 SLC 2.2 polygons in our study area. Using the equation above each polygon has a surface soil carbon and 100-cm soil carbon value. For surface soil carbon, the values range from 0-212 t C/ha and the weighted average is 108 t C/ha. For 100-cm soil carbon, the values range from 0-751 t C/ha) and the weighted average is 357 t C/ha.

2.3   Peatland Soil Carbon

2.3.1   Peat carbon stocks

Oil sands production occurs primarily in boreal forest regions with abundant peat-accumulating and carbon-rich wetlands including rainwater-fed bogs and groundwater-fed fens. However, high-quality and high-resolution estimates of peatland cover and carbon stock variables are not avaiable for our study area. Therefore, we estimate peatland soil carbon values based on the study by Beilman, Vitt et al. (*5*). Beilman, Vitt et al. (*5*) contains high-resolution wetland map data, a synthesis of available peat carbon characteristic and peat depth datasets, and geostatistical estimates of organic carbon stocks in peatlands of a study area neighboring the oil sands region. A wetland inventory of both peatlands and nonpeat-accumulating wetlands was created for the study area from aerial photographs of 1: 15 000–1: 40 000 scale, and the classification of vegetation and physiography according to Halsey, Vitt et al. (*13*). Three generalized peatland types were considered: treed bogs, treed fens (wooded fens), and open fens (treeless, including both shrub- and sedge-dominated fens).

Beilman, Vitt et al. (*5*) found that peatlands cover around 32% of their 25,119 km^2 study area, and consist mainly treed fen peatlands (52% of total peatland area), followed by bog area (38%). The thickness of peat deposits measured at 203 sites was 2.5m on average but as deep as 6m, and highly variable between sites.

The peat carbon stock estimate for the Beilman, Vitt et al. (*5*) study area yielded 982–1025 Tg C. Polygon-scale peat carbon mass per unit area ranged from 530 to 1650 t C/ha. The difference between different peatland classifications are small, with the mean carbon values for bogs, treed fens, and opened fens 1155, 1189, and 1192 t C/ha, respectively. Overall, the mean carbon value for peat estimated for Mackenzie Basin study area is 1180 t C/ha (*14*); a value similar to previous study for Alberta boreal forest region of 1213 t C/ha (*11*). We assume that these carefully studied values from a neighboring region are similar to our oil sands study area, and adopt the same mean total belowground carbon value for peatlands of 1180 t C/ha.

2.3.2 Alberta Wetland Inventory Classification System Version 2.0

Peatland coverage within our study area are estimated from the coarse inventory maps of Vitt, Halsey et al. (*4*) which consists of the percent peatland coverage of 14992 polygons for the province of Alberta. No information on the specific location of individual peatlands within a polygon is provided. Peatlands and peatland complexes across Alberta were inventoried by type from 1: 40 000 to 1: 60 000 aerial photographs following the classification of Halsey, Vitt et al. , and the data were summarized at 1: 250 000. At this scale, individual peatlands were rarely identified, with most polygons composed of peatland complexes and the components identified to the nearest 10% cover. s. Areal extents as percentages were calculated in ARC/INFO for 0.25° latitude and 0.5° longitude grids by peatland type.

Peatland area was calculated for the oil sands study area based on the assumption that LUC polygons for all forest classes calculated from change detection results could be associated with % peatland cover values from Vitt, Halsey et al. (*4*). LUCs include conversions of mixed forest/peatland, coniferous forests, broadleaf forests to bare soil and water, and conversion of bare soil to water. Therefore, each disturbed polygon can include peat area and non-peat area.

For the areas calculated as peatland, we applied the belowground peatland carbon value of 1180 t C/ha from Beilman, Vitt et al. (2008). For areas calculated as non-peatland, we applied soil carbon values from The Soil Landscapes of Canada (SLC 2.2).

2.4   Post-Disturbance Carbon Losses

2.4.1   Percentage of Soil C loss (F_{soil})

Surface mining involves the draining of land and the clearing of vegetation, as well as the removal of soil including peat. Subsoil and overburden[1] are removed and stored separately. Disturbed soil is stockpiled and stored until reclamation, and peat stockpiles may be used subsequently as a soil amendment (*16*). The drained and/or extracted soil will experience some destabilization of its organic matter and will decompose to some degree, releasing CO_2. Peat soils in particular can contain a very large amount of organic carbon and can also lead to emissions of CH_4, a more potent greenhouse gas than CO2,depending on moisture conditions (*17*).

Some peer-reviewed articles assume all stored C, including peat, will eventually decompose and releasing back to the atmosphere after disturbance (*18, 19*). Empirical data and observations of soil carbon loss after disturbance from oil sands production are scant. Rooney, Bayley et al. (*20*) reported that postmining soils contains soil C values between 50 and 146 t C/ha (*21*) which is less than the weighted average of soil carbon storage of 357 t C/ha for the oil sands regions suggested by SLC 2.2 and substantially less than the range of soil carbon in carbon-rich peatlands of 530-1650 t C/ha observed by (*5*) in their nearby study area. The prescribed soil carbon values are up to 86% less than the SLC 2.2 weighted average and up to 97% less than the maximum soil carbon values in peatland soils. We use 90% as a first approximation estimate and an uncertainty range of 50-95% for surface mining soil C loss.

The type of land use disturbance associated with in-situ production include exploration well, cutline, 2D and 3D seismic delineation, production well, well pads, well sets, roads, pipeline and production plants (*22*). Soils disturbed by these land uses can also destabilize soil organic matter and promote decomposition and release of CO_2.

A recent meta-analysis of global pattern of soil carbon losses from the conversion of forests to agricultural land found a mean loss factor of 31% decrease in the soil organic carbon stock after disturbance in the boreal region for the top 30 cm soil C stock measured (*23*). The majority of the studies included in the meta analysis (*23*) do not measure soil carbon loss beyond 30 cm there estimates of soil carbon loss factor beyond 30 cm were not reported in the study. We use soil carbon loss factor (F_{soil}) of 20-40% for the in-situ production for surface soil C (<30 cm). We do not have measures for surface (<30 cm) soil C values for peatland though it is known that 1/3 of peatland soil C is stored at the top 1 m. We therefore assume that the ratio between forest surface soil C <30 cm and 1 m (average of 114.35 tC/ha and 384.4 tC/ha = 0.29)

---

[1] Overburden is a layer of sand, gravel and shale between the surface and the underlying oil sand. Overburden must be removed before oil sands can be mined.

is the same for peatland soil. Based on these, we assume that 10% of peatland soil C resides above 30 cm.

2.4.2 Percentage of Biomass C loss (F$_{bio}$)

Our study uses two approaches to account for biomass carbon loss after conversion: (1) a complete loss after conversion and (2) accounting for carbon storage in harvested wood products (HWP) and solid waste disposal site (SWDS) based on the calculation in Earles, Yeh et al. (*24*). Earles, Yeh et al. (*24*) estimate that the average amount of biomass carbon stored in HWP and SWDS stocks for Canada are 50%, 28%, and 20% in 0, 30 and 50 years after harvest, respectively. Based on these two approaches we assume 72-100% of biomass carbon will be lost to the atmosphere within 30 years after disturbance.

2.5   *Foregone Sequestration (Seq$_i$)*

By removing the functional vegetation layer at the surface of a peatland, the disturbed ecosystem loses its ability to sequester CO_2 from the atmosphere. The foregone sequestration refers to the amount of carbon that would have been sequestrated had a GHG sink not been cleared for oil sands production. Once a forest is cleared, it is foregone forever until it is reclaimed back to forest to resequester carbon again. Therefore we can set the value of T to be 100 years or greater. The longer T is assumed, the bigger foregone sequestration value is. To be consistent with many lifecycle analyses particularly those used for fuel regulations in California, US and EU (*25-27*) which typically use a 20-30 years of timeframe of analysis depending on their policy framework. We select T = 50 for surface mining projects and T = 30 for in-situ projects to roughly cover the lifetime of the projects that capture the foregone sequestration using the long-term sequestration rate of mature forests.

Canadian forests have been shown to provide a net sink for carbon through much of this century. But it was shown by Kurz and Apps (1999) that there has been a decrease in this sink since the late 1990's due to increased disturbance such as fire and disease outbreak, such that Canadian forests may now be a net source of carbon or a very small sink (*28*). Others suggest that Canadian boreal deciduous forests can still be a net carbon sink sequestering 1.3 – 2 t C/ha/yr (*29*) or a small sink with an overall trend of increasing biomass and carbon sink (*9, 30*). Pan, Birdsey et al. (*31*) estimated the global annual change in C stock by country or region and concluded that Canada's boreal forest still remains a net sink of 0.11 t C/ha/yr between 1990 and 1999, and a net sink of 0.04 t C/ha/yr between 2000 and 2007.

Peatlands still remain a long-term carbon sink with annual carbon accumulation rate (accounting for historical fires) of 0.24-0.77 t C/ha/yr across continental western Canada (*18, 19*).

Given our study period (1985-2009), we choose not to use a long-term (i.e. decadal) sequestration rate and select 0.04 t C/ha/yr and 0.77 t C/ha/yr as the foregone sequestration rates for Coniferous and Broadleaf Forest and for Bogs and Fens, respectively.

2.6 Forest Regrowth (REGROW$_{i,j}$)

Instead of using literature-reviewed values to make assumptions about forest re-growth rates and biomass and soil carbon resequestration rate after reclamation (as it was done in Yeh, Jordaan et al. (2010), we use the actual satellite imagery of forest regrowth areas after disturbance and assign these regrown biomass with the same biomass C values in the corresponding biomass category. The biomass value of the reclaimed area classified as having landscape similar to "Peatland" will be the same (35.5 t C/ha) regardless of the pre-disturbed land type.

3.   LUI and Carbon Intensity of LUC Over Projected Project Lifetime

Future LUC impacts if the remaining established reserved were fully developed were estimated by extrapolating the *net (surface mining)/gross (in-situ)* land use impacts vs. *cumulative* production of a project along the log-log linear curve and sum the area underneath the curve up to the total estimated established reserved for each project.

The total projected LUC impacts (Total_LUC$_i$) of project $_i$ is represented as the sum of the area underneath the regression curve:

$$\text{Total\_LUC}_i = \sum_{n=LUo}^{x} e^{aLog(n)+b} \qquad \textit{(Equation 10)}$$

Where,
  LU$_o$ = initial land use impacts where first data point exists;
  a   = regression coefficient of the log-log linear curve; -0.86 for surface mining project and -1.08 for in-situ project;
  b   = constant value of the log-log linear curve; 15.4 for surface mining and 17.1 for in-situ project;
  x   = cumulative production; x = EUR when the Total_LUC$_i$ is to find the total LU impacts over the entire project lifetime.

We adjust LU$_0$ values so the estimated LUC values for each project *i* are calibrated to the observed LUC value in 2009 when x = cumulative production value of 2009.

Once the potential LUC areas (million m^2) are known, we can estimate the total biomass and soil C emissions associated with converting these land. Since we do not know the exact locations of future land use, we use the average land use CI for each project calculated to calculate the total C emissions associated with converting these areas for developing the remaining oil reserves:

> Estimated total C emissions from the development of the total reserves (kt C) =
> Total_LUCi (10^{6}m^2) × Average land use CI (tC/ha)/10
>
> *(Equation 11)*

The carbon intensity of oil sands project for the entire project lifetime can thus be estimated based on the total *projected* carbon emissions from land use disturbance if the total projected energy is fully developed divided by the estimated total energy produced for a given project site:

> Carbon intensity of oil sands project for the entire project lifetime (gCO_2e/MJ) =
> (Land use C emissions to date + Land use C emissions from the development of remaining reserves)(million tC) / (Energy produced to date + Remaining established reserves) (TJ) $\times 10^6 \times 44/12$
>
> *(Equation 12)*

When extrapolating the calculated land use CI for each project to future period, we consider whether it is necessary to make adjustments to two previous assumptions: foregone sequestration and forest regrowth.

Given that all in-situ sites are likely to be fully developed within 30 years, the assumption of using 30 years for calculating foregone sequestration and ignoring forest regrowth within the project sites still seem adequate. Some LUC associated with in-situ production such as seismic activity may revert back to its natural state fair quickly (~10-20 years); others such as central processing plant, upgrader facility, or even well pads, drainage areas, wells are likely to persist on the landscape longer than 30 years.

Surface mining projects are likely to persist on the landscape longer 50-100 years or longer , the assumptions of 50 years of foregone sequestration may be on the conservative side.

3.1 Estimated Future Production

The ERCB (2013) estimates the in-place volumes and established mineable and in situ crude bitumen reserves on both a project and deposit basis. The in-place volumes were determined using geophysical logs, core, and core analyses. Factors were then applied to the **initial mineable volume in place** to determine the **established reserves**. A series of reduction factors were applied to take into account inaccessible bitumen due to environmental protection corridors along major rivers, small isolated ore bodies, and the location of surface facilities (plant sites, tailings ponds, and waste dumps)(ERCB, 2013). A combined mining and extraction recovery factor of 82 percent is applied to this reduced resource volume. This recovery factor reflects the combined loss, on average, of 18 percent of the in-place volume by mining operations and extraction facilities. The resulting initial established reserves for surface mining project sites are shown in Table S1.

For the in-situ projects, data is taken from companies' Annual Information Forms that they are required to report each year. Similar to the initial mineable volume in place for the surface mining projects, estimates were given as the original bitumen resources in place (OBIP), or producible oil in place (POIP), as indicators of resource volumes amenable to recovery. These annual reports also include detailed expected recovery factors for project sites by drainage area, pad, or by pattern and typically range from 40-70%. Table S1 summarizes the aggregated estimates for each project site based on the latest companies' Annual Information Forms.

Table S1. Mineable and in-situ crude bitumen reserves and cumulative production to date (December 31, 2012).
Source: ERCB (2013).

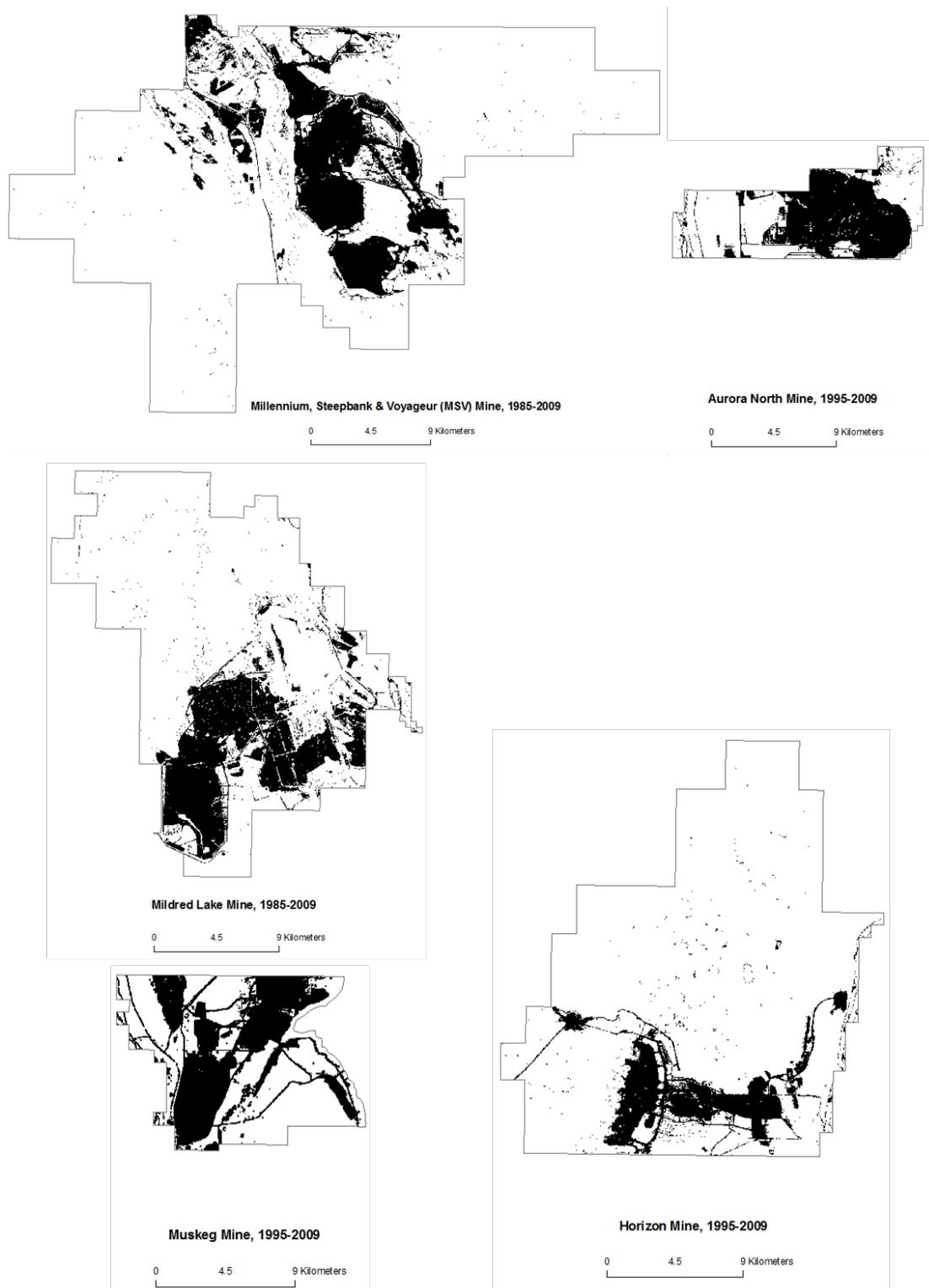| Surface mining projects					
Site	*Initial mineable volume in place $(10^6 m^3)$*	*Initial established reserves (IER) $(10^6 m^3)$*	*% recoverable*	*Cumulative production to date $(10^6 m^3)$*	*% production/IER*
Suncor-MSV mines	990	687	69%	235	34%
Syncrude (Mildred Lake and Aurora North)	2,071	1,306	63%	472	36%
Muskeg and expansion	672	419	62%	84	20%
Horizon	834	537	64%	16	3%
In-situ projects					
	Expected recovery factor	*EUR $(10^6 m^3)$*	*Recovery factor to date*	*Cumulative production to date $(10^6 m^3)$*	*% production/EUR*
Surmont	44%	15.2	19%	5.8	38.3%
Christina Lake	70%	25.8	26%	6.3	24.3%
Mackay River	61%	21.9	37%	13.6	62.3%
Long Lake	57%	28.5	5.5%	6.3	22.0%
Firebag	55%	96.5	14%	23.5	24.3%
Jackfish	66%	27.4	25%	8.3	30.2%
Christina Lake Regional	55%	10.6	28%	4.7	44.3%

Figure S1. Gross land use change of two surface mining projects. Boxes represent project boundaries. Black areas represent gross land use change based on change detection analyses of Landsat imagery as described in detail in the Supporting Information.

S13

Figure S2. Gross land use change of six in-situ projects. Boxes represent project boundaries. Black areas represent gross land use change based on change detection analyses of Landsat imagery as described in detail in the Supporting Information.
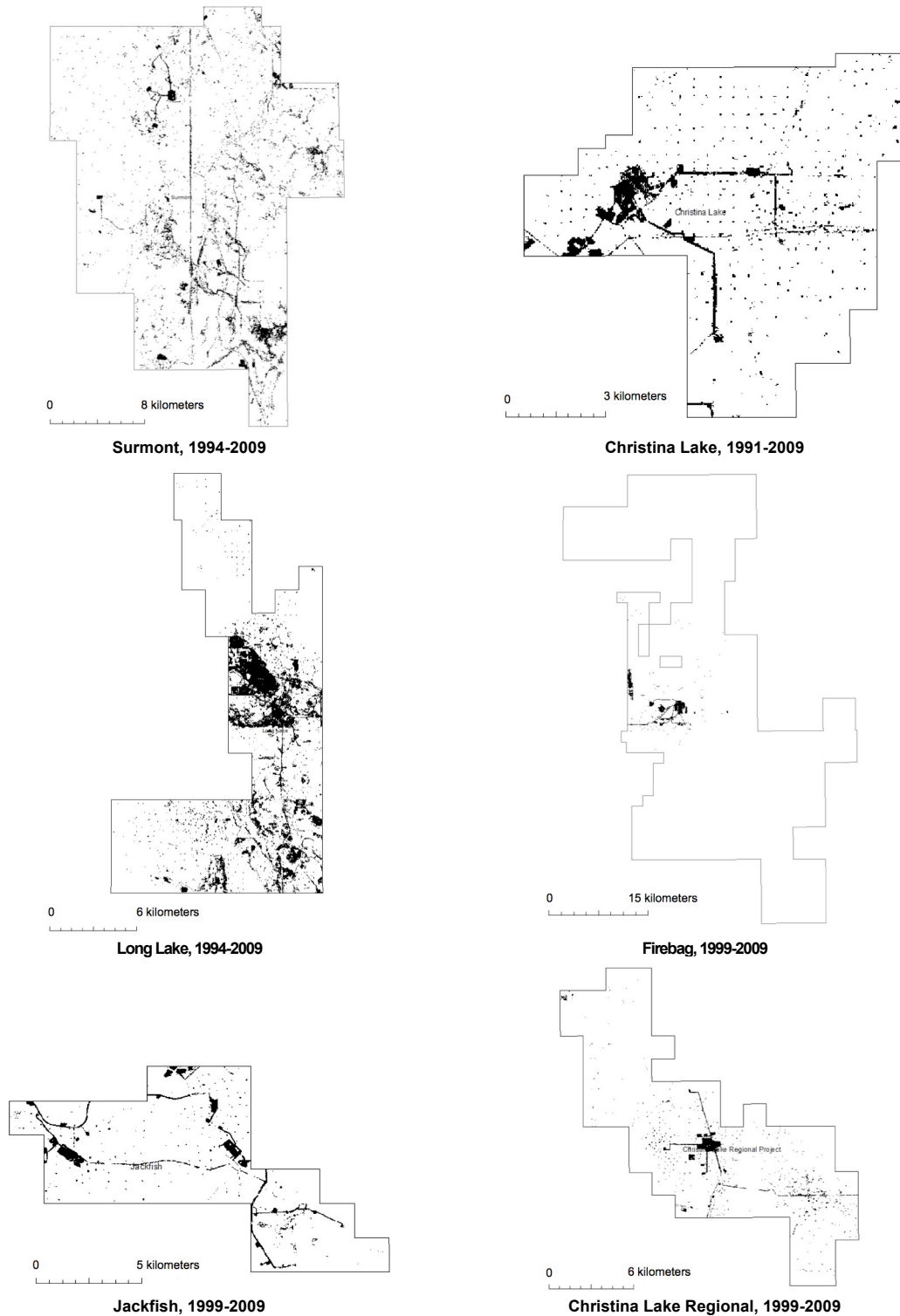
References

1. USGS. (2013).

2. M. J. Canty, *Image Analysis, Classification, and Change Detection in Remote Sensing with algorithms for ENVI/IDL*. (CRC Press/Taylor & Francis, Boca Raton, Florida, 2010).

3. S. N. Gillanders, N. C. Coops, M. A. Wulder, N. R. Goodwin, Application of Landsat satellite imagery to monitor land-cover changes at the Athabasca Oil Sands, Alberta, Canada. *Canadian Geographer / Le Géographe canadien* **52**, 466-485 (2008)10.1111/j.1541-0064.2008.00225.x).

4. D. H. Vitt, L. A. Halsey, M. N. Thormann, T. Martin, Peatland Inventory of Alberta. Phase I: Overview of Peatland Resources in the Natural Regions and Subregions of Alberta. 1996.

5. D. W. Beilman, D. H. Vitt, J. S. Bhatti, S. Forest, Peat carbon stocks in the southern Mackenzie River Basin: uncertainties revealed in a high-resolution case study. *Global Change Biology* **14**, 1-12 (2008)doi: 10.1111/j.1365-2486.2008.01565.x).

6. SLC, "Soil Landscapes of Canada v. 2.2," (Centre for Land and Biological Resources Research. Research Branch, Agriculture and Agri-food Canada, Ottawa, Canada, 1996).

7. J. G. Englander, A. R. Brandt, "Oil Sands Energy Intensity Analysis for GREET Model Update," (Department of Energy Resources Engineering, Stanford University, 2014).

8. IPCC, Ed., *Land Use, Land-Use Change and Forestry*, (Cambridge University Press, Cambridge, England, 2000).

9. G. E. Banfield, J. S. Bhatti, H. Jiang, M. J. Apps, Variability in regional scale estimates of carbon stocks in boreal forest ecosystems: results from West-Central Alberta. *For. Ecol. Manage.* **169**, 15-27 (2002); published online Epub9/15/ (http://dx.doi.org/10.1016/S0378-1127(02)00292-X).

10. J. S. Bhatti, R. C. Errington, I. E. Bauer, P. A. Hurdle, Carbon stock trends along forested peatland margins in central Saskatchewan. *Canadian Journal of Soil Science* **86**, 321-333 (2006); published online Epub2006/03/01 (10.4141/S05-085).

11. D. H. Vitt, L. A. Halsey, I. E. Bauer, C. Campbell, Spatial and temporal trends in carbon storage of peatlands of continental western Canada through the Holocene. *Can. J. Earth Sci.* **37**, 683-693 (2000).

12. R. Plevin, H. Gibbs, J. Duffy, S. Yui, S. Yeh, "Agro-ecological Zone Emission Factor (AEZ-EF) Model (v47)," (GTAP Technical Paper No. 4346, 2014).

13. L. A. Halsey, D. H. Vitt, D. Beilman, S. Crow, S. Mehelcic, R. Wells, "Alberta Wetland Inventory Classification System Version 2.0," (Alberta Sustainable Resource Development, 2004).

14. D. W. Beilman, D. H. Vitt, J. S. Bhatti, S. Forest, Peat carbon stocks in the southern Mackenzie River Basin: Uncertainties revealed in a high-resolution case study. *Global Change Biology* **14**, 1221-1232 (2008).

15. L. Halsey, D. Vitt, S. Zoltai, Climatic and physiographic controls on wetland type and distribution in Manitoba, Canada. *Wetlands* **17**, 243-262 (1997).

16. D. H. Vitt, C. Hayes, K. Wieder, Reclamation of decommissioned oil and gas pads initially constructed in boreal peatlands. *Canadian reclamation : an official publication of the Canadian Land Reclamation Association* **12**, 12-18 (2012).

17. J. Cleary, N. T. Roulet, T. R. Moore, Greenhouse Gas Emissions from Canadian Peat Extraction, 1990-2000: A Life-cycle Analysis. *AMBIO: A Journal of the Human Environment* **34**, 456-461 (2005); published online EpubAugust 01, 2005 (

18. R. K. Wieder, M. A. Vile, K. D. Scott, D. H. Vitt, E. Brault, M. Harris, S. B. Mowbray, in *Restoration and reclamation of boreal ecosystems : attaining sustainable development* D. H. Vitt, J. S. Bhatti, Eds. (Cambridge University Press, Cambridge ; New York, 2012).

19. M. Turetsky, K. Wieder, L. Halsey, D. Vitt, Current disturbance and the diminishing peatland carbon sink. *Geophys. Res. Lett.* **29**, 1526, doi:1510.1029/2001GL014000 (2002).

20. R. C. Rooney, S. E. Bayley, D. W. Schindler, Oil sands mining and reclamation cause massive loss of peatland and stored carbon. *Proceedings of the National Academy of Sciences* **109**, 4933-4937 (2012); published online EpubMarch 27, 2012 (10.1073/pnas.1117693108).

21. Cumulative Effects Management Association, "Results from Long Term Soil and Vegetation Plots Established in the Oil Sands Region (2009): Soils Component," (Paragon Soil and Environmental Consulting, Edmonton, AB, 2010).

22. S. M. Jordaan, D. W. Keith, B. Stelfox, Quantifying land use of oil sands production: a life cycle perspective. *Environmental Research Letters* **4**, 024004 (2009).

23. X. Wei, M. Shao, W. Gale, L. Li, Global pattern of soil carbon losses due to the conversion of forests to agricultural land. *Scientific Reports* **4**, 4062 (2014)10.1038/srep04062).

24. J. M. Earles, S. Yeh, K. E. Skog, Timing of carbon emissions from global forest clearance. *Nature Climate Change*, (2012)10.1038/NCLIMATE1535).

25. U.S. EPA, "Renewable Fuel Standard Program (RFS2) Regulatory Impact Analysis (EPA-420-R-10-006)," (U.S. Environmental Protection Agency, 2010).

26. CARB, "Staff Report: Proposed Regulation to Implement the Low Carbon Fuel Standard—Initial Statement of Reasons. Volume1: Staff Report," (California Air Resources Board, 2009).

27. *European Commission DIRECTIVE 2009/30/EC Amendment to Directive 98/70/EC on environmental quality standards for fuel (Fuel Quality Directive)* (2009 http://eur-lex.europa.eu).

28. W. A. Kurz, M. J. Apps, A 70-Year Retrospective Analysis of Carbon Fluxes in the Canadian Forest Sector. *Ecological Applications* **9**, 526-547 (1999).

29. W. J. Chen, T. A. Black, P. C. Yang, A. G. Barr, H. H. Neumann, Z. Nesic, P. D. Blanken, M. D. Novak, J. Eley, R. J. Ketler, R. Cuenca, Effects of climatic variability on the annual carbon sequestration by a boreal aspen forest. *Global Change Biology* **5**, 41-53 (1999)10.1046/j.1365-2486.1998.00201.x).

30. A. L. Dunn, C. C. Barford, S. C. Wofsy, M. L. Goulden, B. C. Daube, A long-term record of carbon exchange in a boreal black spruce forest: means, responses to interannual variability, and decadal trends. *Global Change Biology* **13**, 577-590 (2007)10.1111/j.1365-2486.2006.01221.x).

31. Y. Pan, R. A. Birdsey, J. Fang, R. Houghton, P. E. Kauppi, W. A. Kurz, O. L. Phillips, A. Shvidenko, S. L. Lewis, J. G. Canadell, P. Ciais, R. B. Jackson, S. W. Pacala, A. D. McGuire, S. Piao, A. Rautiainen, S. Sitch, D. Hayes, A Large and Persistent Carbon Sink in the World's Forests. *Science* **333**, 988-993 (2011); published online EpubAugust 19, 2011 (10.1126/science.1201609).